

AD-A241 656



AEROSPACE REPORT NO.
TOP SECRET (075)-1

2

CO Energy Transfer Processes in the Mesosphere and Thermosphere

Prepared by

V. I. LANG

Space and Environment Technology Center
Technology Operations

15 August 1991

Prepared for

PHILLIPS LABORATORY
GEOPHYSICS DIRECTORATE
Hanscom AFB, MA 01731

SPACE SYSTEMS DIVISION
AIR FORCE SYSTEMS COMMAND
Los Angeles Air Force Base
P. O. Box 92960
Los Angeles, CA 90009-2960

DTIC
ELECTRONIC
OCT 18 1991
S B D

Contract No. F04701-88-C-0089

Engineering and Technology Group

91-13497



THE AEROSPACE CORPORATION
El Segundo, California



APPROVED FOR PUBLIC RELEASE;
DISTRIBUTION UNLIMITED

91 1017 042

TECHNOLOGY OPERATIONS

The Aerospace Corporation functions as an "architect-engineer" for national security programs, specializing in advanced military space systems. The Corporation's Technology Operations supports the effective and timely development and operation of national security systems through scientific research and the application of advanced technology. Vital to the success of the Corporation is the technical staff's wide-ranging expertise and its ability to stay abreast of new technological developments and program support issues associated with rapidly evolving space systems. Contributing capabilities are provided by these individual Technology Centers:

Electronics Technology Center: Microelectronics, solid-state device physics, VLSI reliability, compound semiconductors, radiation hardening, data storage technologies, infrared detector devices and testing; electro-optics, quantum electronics, solid-state lasers, optical propagation and communications; cw and pulsed chemical laser development, optical resonators, beam control, atmospheric propagation, and laser effects and countermeasures; atomic frequency standards, applied laser spectroscopy, laser chemistry, laser optoelectronics, phase conjugation and coherent imaging, solar cell physics, battery electrochemistry, battery testing and evaluation.

Mechanics and Materials Technology Center: Evaluation and characterization of new materials: metals, alloys, ceramics, polymers and their composites, and new forms of carbon; development and analysis of thin films and deposition techniques; nondestructive evaluation, component failure analysis and reliability; fracture mechanics and stress corrosion; development and evaluation of hardened components; analysis and evaluation of materials at cryogenic and elevated temperatures; launch vehicle and reentry fluid mechanics, heat transfer and flight dynamics; chemical and electric propulsion; spacecraft structural mechanics, spacecraft survivability and vulnerability assessment; contamination, thermal and structural control; high temperature thermomechanics, gas kinetics and radiation; lubrication and surface phenomena.

Space and Environment Technology Center: Magnetospheric, auroral and cosmic ray physics, wave-particle interactions, magnetospheric plasma waves; atmospheric and ionospheric physics, density and composition of the upper atmosphere, remote sensing using atmospheric radiation; solar physics, infrared astronomy, infrared signature analysis; effects of solar activity, magnetic storms and nuclear explosions on the earth's atmosphere, ionosphere and magnetosphere; effects of electromagnetic and particulate radiations on space systems; space instrumentation; propellant chemistry, chemical dynamics, environmental chemistry, trace detection; atmospheric chemical reactions, atmospheric optics, light scattering, state-specific chemical reactions and radiative signatures of missile plumes, and sensor out-of-field-of-view rejection.

UNCLASSIFIED

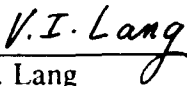
SECURITY CLASSIFICATION OF THIS PAGE

REPORT DOCUMENTATION PAGE

1a. REPORT SECURITY CLASSIFICATION Unclassified		1b. RESTRICTIVE MARKINGS	
2a. SECURITY CLASSIFICATION AUTHORITY		3. DISTRIBUTION/AVAILABILITY OF REPORT Approved for public release; distribution unlimited.	
2b. DECLASSIFICATION/DOWNGRADING SCHEDULE			
4. PERFORMING ORGANIZATION REPORT NUMBER(S) TOR-0091(6078)-1		5. MONITORING ORGANIZATION REPORT NUMBER(S)	
6a. NAME OF PERFORMING ORGANIZATION The Aerospace Corporation Technology Operations	6b. OFFICE SYMBOL (If applicable)	7a. NAME OF MONITORING ORGANIZATION Space Systems Division	
6c. ADDRESS (City, State, and ZIP Code) El Segundo, CA 90245-4691		7b. ADDRESS (City, State, and ZIP Code) Los Angeles Air Force Base Los Angeles, CA 90009-2960	
8a. NAME OF FUNDING/SPONSORING ORGANIZATION Phillips Laboratory	8b. OFFICE SYMBOL (If applicable)	9. PROCUREMENT INSTRUMENT IDENTIFICATION NUMBER F04701-88-C-0089	
8c. ADDRESS (City, State, and ZIP Code) Geophysics Directorate Hanscom AFB, MA 01731		10. SOURCE OF FUNDING NUMBERS	
		PROGRAM ELEMENT NO.	PROJECT NO.
		TASK NO.	WORK UNIT ACCESSION NO.
11. TITLE (Include Security Classification) CO Energy Transfer Processes in the Mesosphere and Thermosphere			
12. PERSONAL AUTHOR(S) Lang, Valerie I.			
13a. TYPE OF REPORT	13b. TIME COVERED FROM _____ TO _____	14. DATE OF REPORT (Year, Month, Day) 15 August 1991	15. PAGE COUNT 35
16. SUPPLEMENTARY NOTATION			
17. COSATI CODES		18. SUBJECT TERMS (Continue on reverse if necessary and identify by block number)	
FIELD	GROUP	CO (Carbon Monoxide)	
		Non-Local Thermodynamic Equilibrium	
		Upper Atmosphere	
		Vibrational Relaxation	
19. ABSTRACT (Continue on reverse if necessary and identify by block number) A critical review of rate constants for CO collisional relaxation processes and spontaneous emission processes is presented. Collision partners and vibrational excitation levels are limited to those relevant to the atmosphere between 50 and 300 km under nonlocal thermodynamic equilibrium conditions. The rates discussed are important parameters for modeling atmospheric infrared radiance. Background atmospheric radiation is an important consideration in aerospace sensor design. Accurate models describing the dissipation of radiation entering the earth's atmosphere as sunshine or energetic electrons are also necessary to predict global warming or cooling. The revised rate coefficients have been incorporated into the Strategic High Altitude Radiance Code (SHARC) 2.0, 1991.			
20. DISTRIBUTION/AVAILABILITY OF ABSTRACT <input type="checkbox"/> UNCLASSIFIED/UNLIMITED <input checked="" type="checkbox"/> SAME AS RPT <input type="checkbox"/> DTIC USERS		21. ABSTRACT SECURITY CLASSIFICATION Unclassified	
22a. NAME OF RESPONSIBLE INDIVIDUAL		22b. TELEPHONE (Include Area Code)	22c. OFFICE SYMBOL

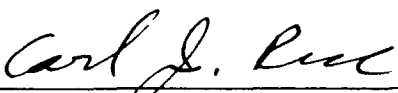
CO ENERGY TRANSFER PROCESSES IN THE MESOSPHERE AND THERMOSPHERE

Prepared



V. I. Lang

Approved



C. J. Rice, Director
Target Signatures and Backgrounds
Department



A. B. Christensen, Principal Director
Space and Environment Technology Center

The information in a Technical Operating Report is developed for a particular program and is not necessarily of broader technical applicability.

PREFACE

This report was prepared with funding and assistance provided by R. D. Sharma, Phillips Laboratory, Geophysics Directorate, Hanscom Air Force Base, MA, as part of the Strategic High Altitude Radiance Code development program.



Accession For	
NTIS GRA&I	<input checked="" type="checkbox"/>
DTIC TAB	<input type="checkbox"/>
Unannounced	<input type="checkbox"/>
Justification	
By	
Distribution/	
Availability Codes	
Dist	Avail and/or Special
A-1	

CONTENTS

PREFACE	1
CO ENERGY TRANSFER PROCESSES IN THE MESOSPHERE AND THERMOSPHERE	5
REFERENCES	13
APPENDIXES	
A. V-V ENERGY TRANSFER FROM CO TO O ₂	15
B. V-V ENERGY TRANSFER FROM CO TO N ₂	21
C. V-T ENERGY TRANSFER FROM CO TO O(³ P)	27
D. V-T ENERGY TRANSFER FROM CO TO O ₂ OR N ₂	33
E. CO SPONTANEOUS EMISSION PROCESSES	39
F. MODEL ATMOSPHERE USED FOR SHARC CALCULATIONS	43

FIGURES

1. Relaxation mechanisms of vibrationally excited CO	6
2. Calculation of CO(2-0) radiance using SHARC 2.0	12

TABLES

1. Revisions to CO Kinetics	8
2. CO Band Radiance Comparison	11

CO ENERGY TRANSFER PROCESSES IN THE MESOSPHERE AND THERMOSPHERE

The original purpose of this review was to update the CO chemical kinetics module in the Strategic High Altitude Radiance Code (SHARC) (Ref. 1). The code contained circa 1974 rate constants for the collisional relaxation of vibrationally excited CO. The source of these rate constants was a review article by Taylor, entitled Energy Transfer Processes in the Stratosphere (Ref. 2).

Since 1974, new experimental techniques have enabled researchers to study the temperature dependence of specific vibrational energy relaxation processes. In particular, laser-induced fluorescence (LIF) studies have filled the gap between room temperature measurements and high temperature shock-tube studies. The data acquired for CO has improved in both quantity and reliability over the past few decades.

For the purpose of this report and for updating SHARC, CO relaxation processes relevant to the thermosphere and mesosphere have been considered. The altitude range covered by the model atmosphere profiles in SHARC (Version 2.0, 1991) is 50 to 300 km. Over this altitude span, the density of molecules decreases dramatically, so the number of collisions also decreases. For vibrationally excited species that are potential infrared radiators, spontaneous emission processes become *competitive* with nonradiative collisional deactivation; that is, the system begins to deviate from local-thermodynamic equilibrium (LTE). Generally, if there are less than a million collisions in a radiative lifetime $1/A$, where A is the Einstein coefficient for spontaneous emission, then the system is non-LTE (Ref. 3). In order to fully characterize the atmospheric, non-LTE processes of CO, the Einstein A coefficients for each relevant vibrational level have also been reviewed.

The available literature (through 1990) was evaluated for each of the following collisional deexcitation pathways, where $v = 1$ or 2 :



In the case of O_2 and N_2 as collision partners, both V-V and V-T relaxation mechanisms were considered. The relative spacing of the vibrational energy levels of CO, O_2 , and N_2 is illustrated in Figure 1.

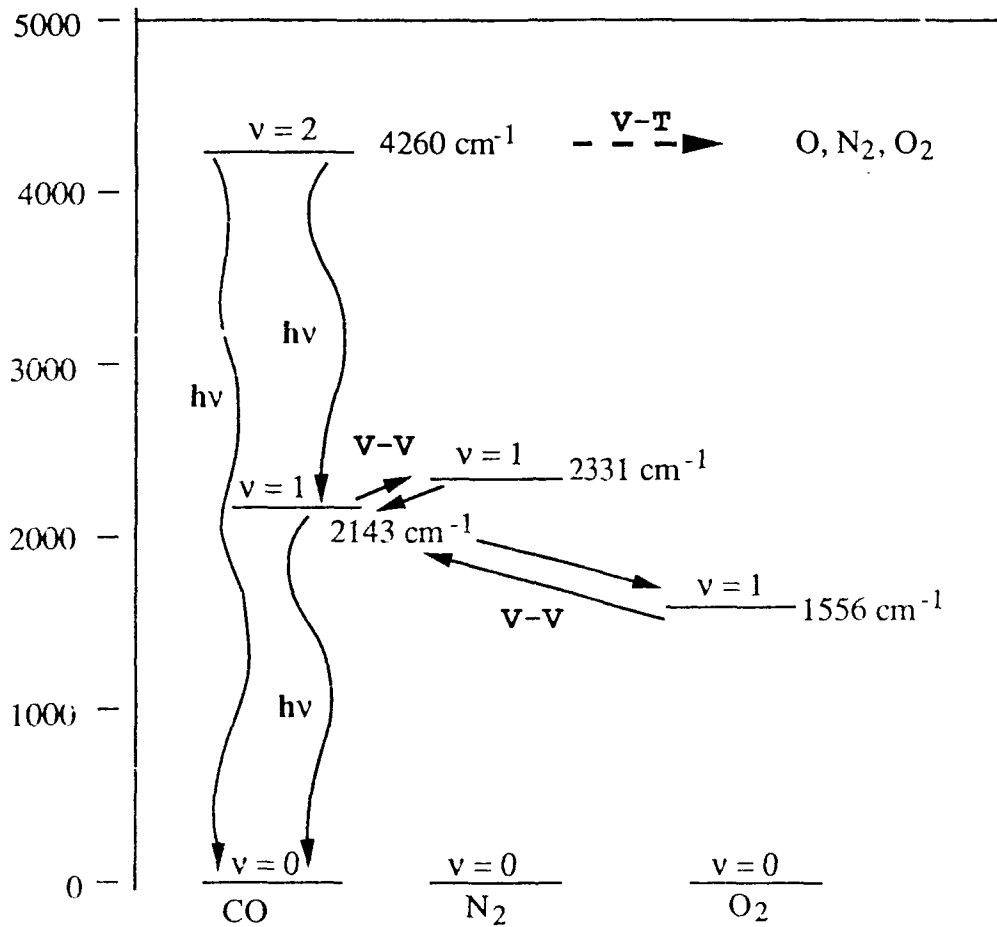


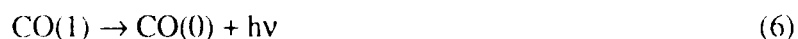
Figure 1. Relaxation mechanisms of vibrationally excited CO.

Ambient temperatures between approximately 190 and 1300 K are common to the altitude range from 50 to 300 km. The lowest temperatures are likely to be found in the 85-90 km altitude layer at arctic latitudes, while the highest temperatures that occur at the top of the atmosphere (300 km in SHARC) are produced during episodes of high solar activity. A common functional form for the temperature dependence of the rate constants for collisional deexcitation (and excitation) reactions is desirable for modeling purposes. The following form, used by SHARC and adopted in this review, is based on the theory of Landau and Teller (Ref. 4):

$$k = A_i \exp(-B_i/T^{1/3} - C_i/T) \quad (5)$$

The $T^{-1/3}$ dependence arises from the expression for the most probable velocity for an effective energy transfer collision (Refs. 4, 5). In the present analysis of experimental rate constant data, plots of $\ln k$ vs. $T^{-1/3}$ were used to establish linear trends that can be extrapolated or interpolated to temperatures of atmospheric relevance. The $-C_i/T$ factor in Eq. (5) was added to the exponential term to describe processes that have an energy defect. If the energy transfer process is endothermic, $C_i = \Delta E$; otherwise, $C_i = 0$. The collisional relaxation data are compiled in Appendices A-D. The original references are listed with the appendices.

The spontaneous emission processes that can occur from the CO $v=1$ or $v=2$ vibrational levels are



The unimolecular rate constants for these decay processes can be calculated from the appropriate rovibrational band strength or the transition dipole moment. In order to standardize all of these rates, the most recent sum-of-lines band strengths from the Atmospheric Trace Molecule Spectroscopy (ATMOS) (Ref. 6) high resolution data base have been used to calculate the Einstein A coefficients for the processes described by Eqs. (6)-(8). These values, as well as references to the spectroscopic literature, are given in Appendix E.

Table 1 summarizes the recommended changes to the rate constants for both the radiative and nonradiative processes. CO radiance calculations were performed with SHARC using both the old (1974) collisional relaxation rates and the revised (1990)

Table 1. Revisions to CO Kinetics

V-T Reactions ^{(c),(d)}	Coefficients (1974 Data) ^(a)			Revised Coefficients ^(a)		
	A _i	B _i	C _i ^(b)	A _i	B _i	C _i ^(b)
M + CO(1) - M + CO(0) N ₂ /1.0/ O ₂ /1.0/	6.67e-08	208.3	0.0	9.90e-09	168.1	0.0
M + CO(0) - M + CO(1) N ₂ /1.0/ O ₂ /1.0/	6.67e-08	208.3	3083.7	9.90e-09	168.1	3083.7
M + CO(2) - M + CO(1) N ₂ /1.0/ O ₂ /1.0/	1.33e-07	208.3	0.0	1.98e-08	168.1	0.0
M + CO(1) - M + CO(2) N ₂ /1.0/ O ₂ /1.0/	1.33e-07	208.3	3045.6	1.98e-08	168.1	3045.6
M + CO(2) - M + CO(0) N ₂ /1.0/ O ₂ /1.0/	1.33e-07	208.3	0.0	1.98e-09	336.2	0.0
M + CO(0) - M + CO(2) N ₂ /1.0/ O ₂ /1.0/	1.33e-07	208.3	6129.3	1.98e-09	336.2	6129.3
O + CO(1) - O + CO(0)	9.90e-08	118.1	0.0	2.82e-09	75.4	0.0
O + CO(0) - O + CO(1)	9.90e-08	118.1	3083.7	2.82e-09	75.4	3083.7
O + CO(2) - O + CO(1)	1.98e-07	118.1	0.0	5.64e-09	75.4	0.0
O + CO(1) - O + CO(2)	1.98e-07	118.1	3045.6	5.64e-09	75.4	3045.6
O + CO(2) - O + CO(0)	1.98e-07	118.1	0.0	5.64e-10	150.8	0.0
O + CO(0) - O + CO(2)	1.98e-07	118.1	6129.3	5.64e-10	150.8	6129.3

Table 1. Revisions to CO Kinetics (continued)

	Coefficients (1974 Data) ^(a)			Revised Coefficients ^(a)			
	A _i	B _i	C _i	A _i	B _i	C _i	
V-V Reactions^(d)							
	CO(0) + N ₂ (1) - CO(1) + N ₂ (0)	6.98e-13	25.6	0.0	9.06e-13	26.8	0.0
	CO(1) + N ₂ (0) - CO(0) + N ₂ (1)	6.98e-13	25.6	268.5	9.06e-13	26.8	268.5
	CO(0) + O ₂ (1) - CO(1) + O ₂ (0)	3.50e-10	124.0	844.4	1.17e-12	61.3	844.4
	CO(1) + O ₂ (0) - CO(0) + O ₂ (1)	3.50e-10	124.0	0.0	1.17e-12	61.3	0.0
hν Emission^(e)							
	CO(1) - CO(0) + hν	30.96	0.0	0.0	33.98	0.0	0.0
	CO(2) - CO(1) + hν	60.45	0.0	0.0	64.43	0.0	0.0
	CO(2) - CO(0) + hν	1.03	0.0	0.0	0.922	0.0	0.0

(a) Function $k = A_i \exp(-B_i T^{-1/3} - C_i T^{-1})$.

(b) $D_i = \Delta E \text{ (cm}^{-1}\text{)}/1.44$.

(c) Efficiencies of collision partner are listed below each reaction.

(d) Rate units are $\text{cm}^3 \text{ molecule}^{-1} \text{ s}^{-1}$.

(e) Rate units are s^{-1} .

collisional relaxation rates. The small changes made to the Einstein A coefficients (see Table 1) were not included in the calculation. An equatorial atmosphere that represented relatively high solar and geomagnetic activity was constructed using the Mass Spectrometer and Incoherent Scatter (MSIS) 1983 model (Ref. 7) and the SHARC 1976 Standard Atmosphere (Ref. 1). This particular atmosphere, which features high O atom densities at altitudes > 86 km, was chosen for its sensitivity towards changes in the CO kinetics. A listing of the atmosphere is provided in Appendix F. Using this model atmosphere for the starting molecular number densities, SHARC calculated excited state populations for CO. The other species included in the atmosphere were H, O, N₂, O₂, H₂O, OH, NO, CO₂, and O₃. The results of the comparison are given in Table 2. The overall effect of the revisions was an increase in the intensity of the (1-0) band at the expense of the (2-1) and (2-0) bands. The total band radiance for the three bands was essentially constant. Since the (2-1) and (2-0) are much weaker than the (1-0) band, a factor of 100 change in the hot and overtone bands resulted in only a 10% difference in the (1-0) band. The effect on the CO (2-0) emission band is illustrated in Figure 2. The diagram compares the radiance calculated by SHARC using the set of rate constants proposed by Taylor (Ref. 2) with that calculated using the rate constants listed in this review (Table 1).

The experimental data for CO relaxation processes have considerably improved since 1974. The updated temperature dependences calculated in this report should be included in radiance models used for infrared sensor designs covering the 4.7 μm and/or the 2.3 μm regions. Energy transfer rates, including those for CO, are also important parameters in climate models used to calculate the dissipation of sunlight or electron energy entering the Earth's atmosphere. Absorption and reemission of radiation by atmospheric molecules is an important consideration in calculating global temperature trends.

Table 2. CO Band Radiance Comparison^{(a),(b)}

CO Vibrational Band	A Radiance (Taylor, 1974) W/sr/cm ²	B Radiance (Revised Kinetics) W/sr/cm ²	Comparison A/B
(1-0) 2143.27 cm ⁻¹	1.6456e-10	1.8129e-10	0.91
(2-1) 2116.79 cm ⁻¹	1.6378e-11	1.6529e-13	99.1
(2-0) 4260.06 cm ⁻¹	7.0440e-13	7.0969e-15	99.3
TOTAL	1.8164e-09	1.8146e-09	1.00

(a) See Appendix F for Model Atmosphere Listing.

(b) SHARC 2.0 Calculation, 200 km Limb View, 0⁰ Latitude, 0⁰ Longitude.

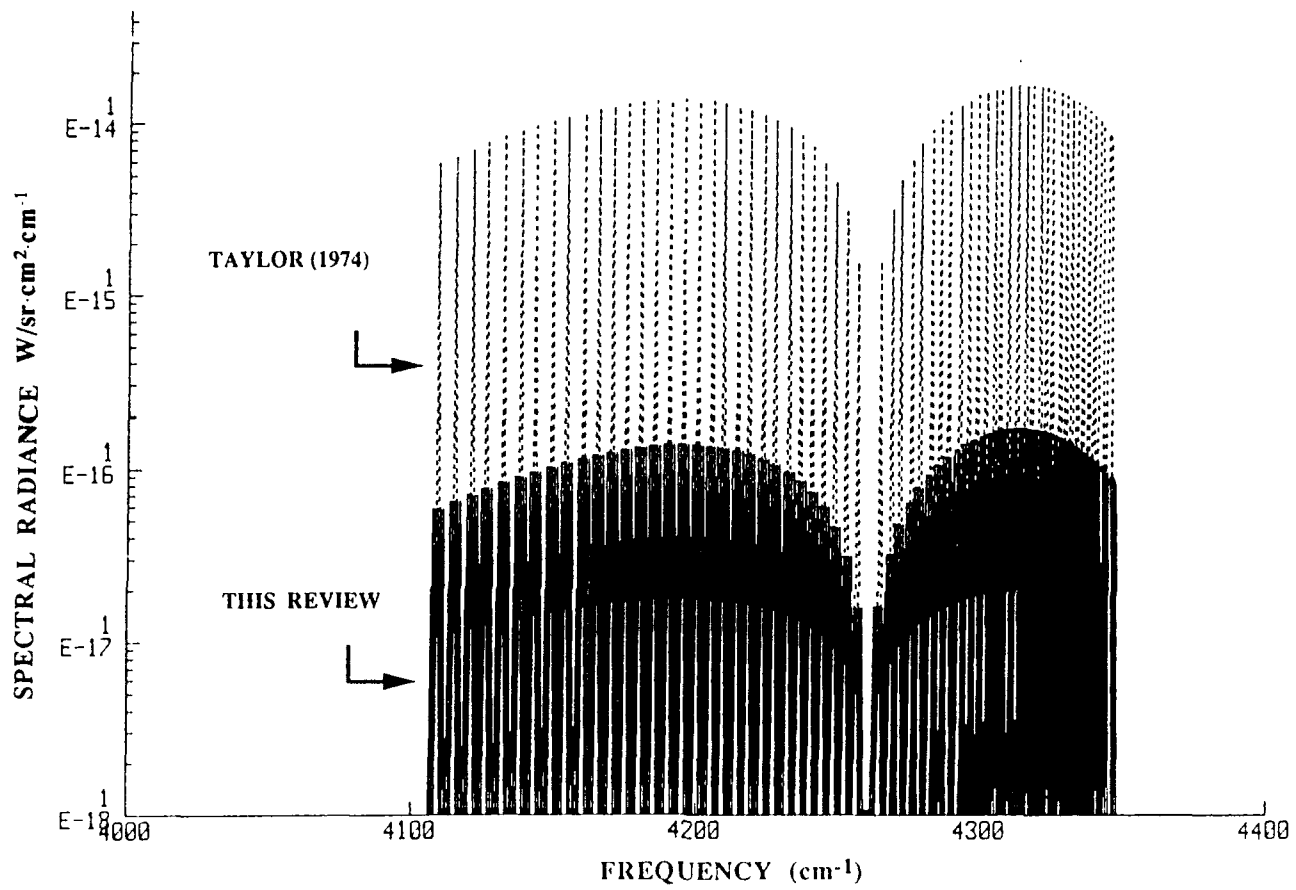


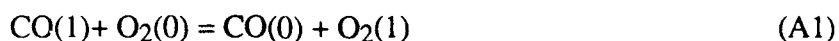
Figure 2. Calculation of CO(2-0) radiance using SHARC 2.0.

REFERENCES

1. R. D. Sharma et al., *SHARC 2.0 (Strategic High Altitude Radiance Code)*, Geophysics Directorate, PL/GP/OP, Hanscom AFB (1991).
2. R. L. Taylor, *Can. J. Chem.*, **52**, 1381 (1974).
3. R. D. Sharma in *Modelling of the Atmosphere*, SPIE Vol. 928, 1988, p. 187.
4. L. Landau and E. Teller, *Phys. Zeit. Sowjetunion*, **10**, 34 (1936).
5. T. L. Cottrell and J. C. McCoubrey, *Molecular Eenergy Transfer in Gases*, (Butterworths: London), 1961, p.141.
6. L. R. Brown et al., *Appl. Opt.*, **26**, 5154 (1987).
7. A. E. Hedin, *J. Geophys. Res.*, **88**, 10,176 (1983).

APPENDIX A: V-V ENERGY TRANSFER FROM CO TO O₂

In the forward direction, the process described by Eq. (A1)



is an exothermic energy transfer process. The energy discrepancy of 587 cm⁻¹ between the CO(1) and O₂(1) levels is too large to classify this process as resonant, even though it occurs between discrete vibrational energy levels of two molecules.

Taylor (Ref. A1) derived the following temperature dependence for Eq. (A1) based on high temperature shock-tube references (Refs. A2, A3):

$$k_{\text{forward}} = 3.50\text{e-}10 \exp(-124.0 T^{-1/3}) \quad (\text{A2})$$

Several more recent temperature dependent studies have been done. Doyennette et al. (Ref. A4) and Gregory et al. (Ref. A5) performed laser-induced fluorescence (LIF) studies, while Miller and Millikan (Ref. A6) used a steady state vibrational quenching technique. The more limited LIF room temperature studies of Green and Hancock (Ref. A7) and the chemiluminescence studies of Hancock and Smith (Ref. A8) overlap with the data of Refs. A4-A6. The data from Refs. A2-A8 are compiled in Figure A1. The Landau-Teller expression obtained from the slope and intercept of Figure A1 is

$$k_{\text{forward}} = 1.17\text{e-}12 \exp(-61.3 T^{-1/3}) \quad (\text{A3})$$

The appropriate reverse rate equation, including the energy difference term, is simply

$$k_{\text{reverse}} = 1.17\text{e-}12 \exp(-61.3 T^{-1/3} - 844.4 T^{-1}) \quad (\text{A4})$$

There is a significant difference between the temperature dependence described by Taylor and the temperature obtained in this analysis, according to Figure A1. The CO to O₂ V-V rates determined experimentally by Refs. A4-A8 are generally faster than those previously predicted by Taylor's extrapolation of high temperature shock-tube data to low temperatures.

At temperatures below ~ 600 K, each of Refs. A4-A6 shows a steep curvature in the Landau-Teller plot. Since the curvature is very different in each set of data, the effect is averaged out in the linear fit of Eq. (A3). References A4 and A5 contain a discussion of

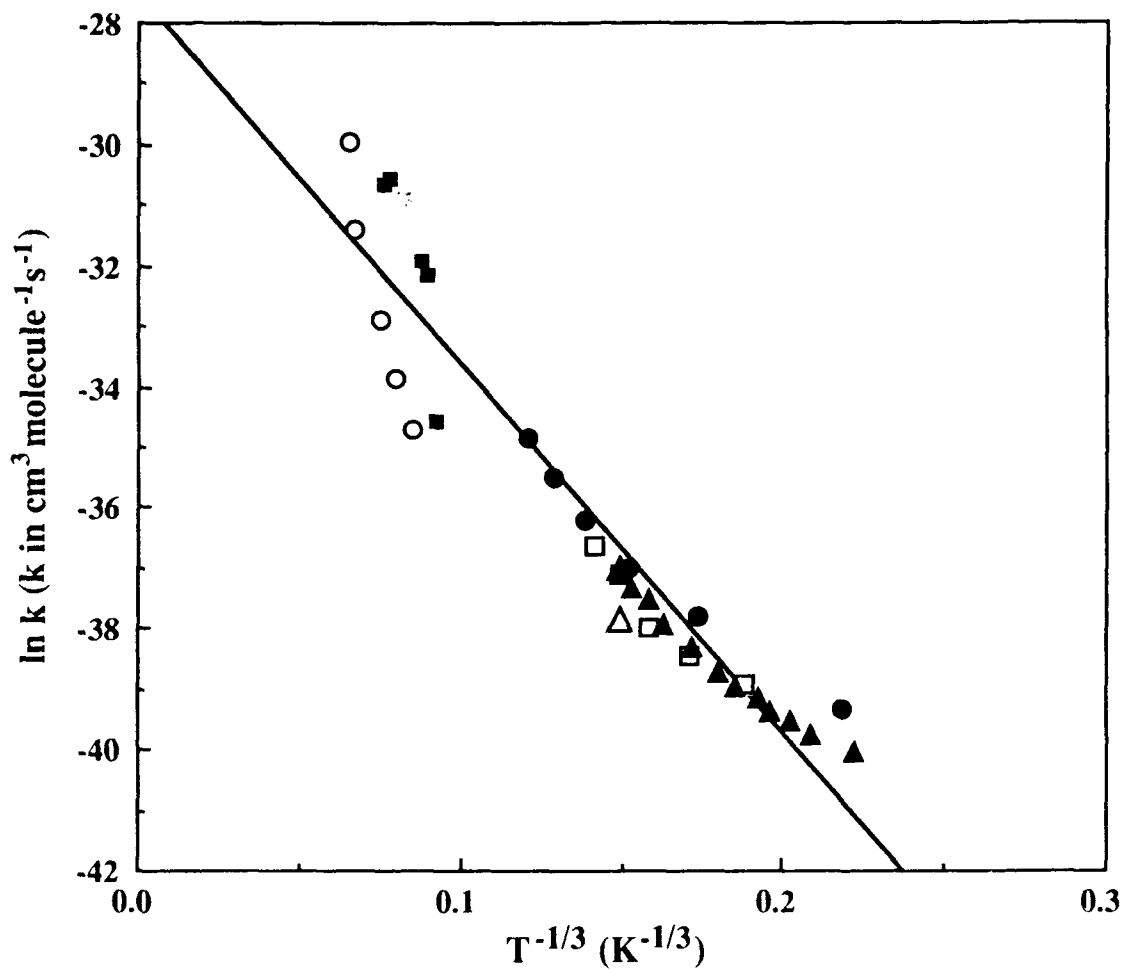


Figure A1. V-V energy transfer from CO(1) to O₂(0). Data from Miller and Millikan (Ref. A6), □; Doyennette et al. (Ref. A4), ●; Hancock and Smith (Ref. A8)/Green and Hancock (Ref. A1), △; Center (Ref. A3), ○; Gregory et al. (Ref. A5), ▲; Sato et al. (Ref. A2), ■.

the importance of short-range intermolecular forces in this type of energy transfer process. Over narrower temperature ranges, different functions of T could provide a better fit to the data.

REFERENCES

- A1. R. L. Taylor, *Can. J. Chem.*, **52**, 1381 (1974).
- A2. Y. Sato, S. Tsuchiya, and K. Koratini, *J. Chem. Phys.*, **50**, 1911 (1969). (1000-3000 K)
- A3. R. E. Center, *J. Chem. Phys.*, **58**, 5230 (1973). (1500-4000 K)
- A4. L. Doyennette et al., *J. Chem. Phys.*, **67**, 3360 (1977). (625-100 K)
- A5. E. Gregory et al., *J. Chem. Phys.*, **78**, 3881 (1983). (90-300 K)
- A6. D. Miller and R. Millikan, *Chem. Phys. Lett.*, **27**, 10 (1974). (300-140 K)
- A7. W. H. Green and J. K. Hancock, *J. Chem. Phys.*, **59**, 4326 (1973). (Room Temperature)
- A8. G. Hancock and I. W. M. Smith, *Appl. Opt.*, **10**, 1827 (1971). (Room Temperature)

APPENDIX B: V-V ENERGY TRANSFER FROM CO TO N₂

The following process is a resonant energy transfer since the CO(1) level occurs only 187.5 cm⁻¹ below the ¹⁴N₂(1) level:



The equation used by Taylor to describe the temperature dependence of the endothermic process was (Ref. B1)

$$k_{\text{forward}} = 6.98\text{e-}13 \exp(-25.60T^{-1/3} - 268.5T^{-1}) \quad (\text{B2})$$

The rate equation for the reverse reaction has the same coefficients without the $\Delta E/T$ term. Four references (B2-B5) were cited by Taylor. Of these, only one room temperature study by Zittel and Moore (Ref. B2) employed the laser-induced fluorescence (LIF) technique. The others were high temperature shock-tube measurements. However, due to this one reliable room temperature measurement, the temperature dependence that Taylor derived [Eq. (B2)] was not appreciably affected by later measurements at temperatures between 70 and 700 K. In the present evaluation, the data from Refs. B2-B5 were combined with newer data from Refs. B6-B11. In Figure B1, $\ln k + 268.5 T^{-1}$ vs. $T^{-1/3}$ is plotted in order to directly fit for the temperature dependence of CO deactivation by N₂. A distinct change in slope occurs at $T^{-1/3} \cong .08$ (i.e., $T \cong 2000$ K). Neither Taylor's Eq. (B1) nor the present fit described by the following equation

$$k_{\text{forward}} = 9.06\text{e-}13 \exp(-26.84T^{-1/3} - 268.5T^{-1}) \quad (\text{B3})$$

includes the measurements for $T > 2000$ K, since temperatures below 2000 K are generally used for atmospheric calculations.

On an expanded $T^{-1/3}$ scale, each set of low temperature results deviates positively from the linear fit, particularly for $T < 200$ K. A discussion of the theoretical basis for the observed temperature trends in the rate of V-V energy exchange between diatomic molecules can be found in Ref. B6. Maricq et al. describe a Morse intermolecular potential that can be used to adequately describe the behavior. However, the low temperature curvature away from Landau-Teller behavior appears to be less than the error limits due to systematic variations between individual experiments. For example, the data of Mastrocinque are somewhat inconsistent with the shape reported in the other references.

Generally, the curvature becomes well defined at temperatures that are lower than those relevant to mesospheric processes, so we have maintained the linear function in $T^{-1/3}$.

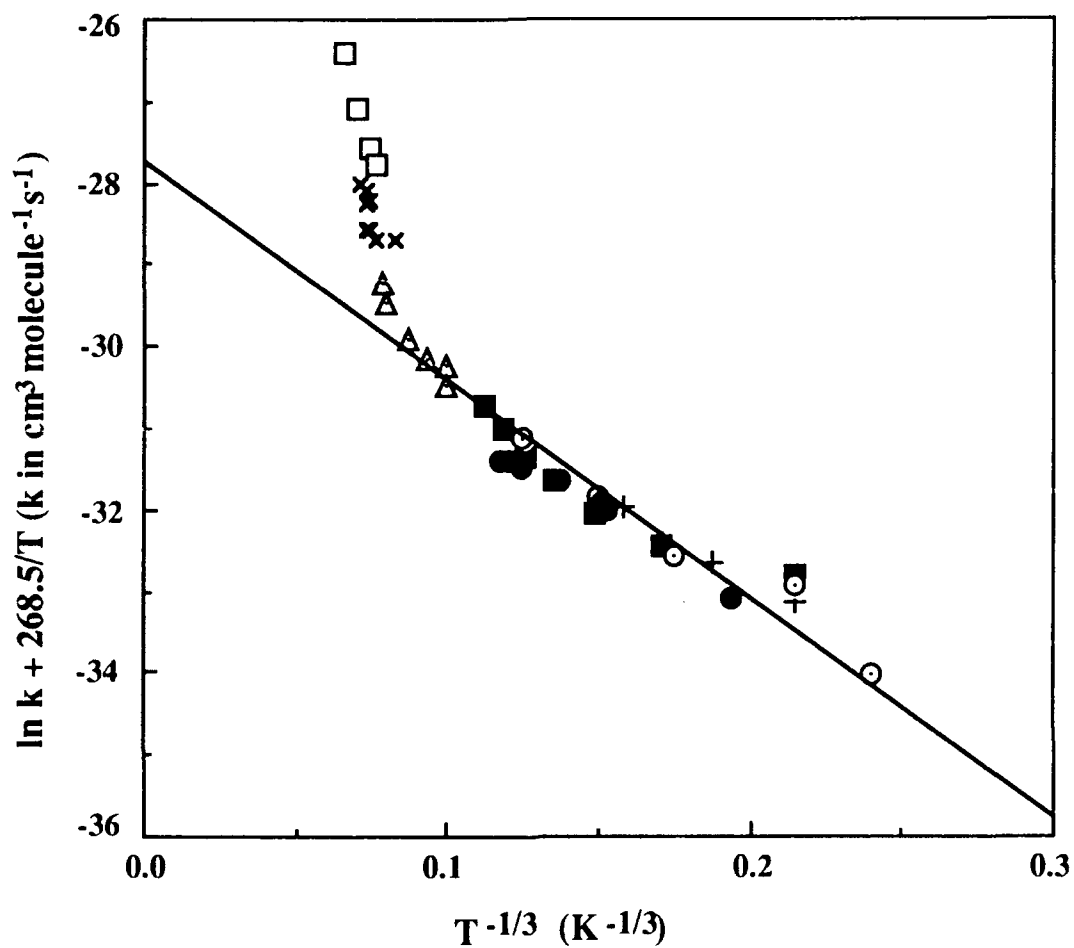


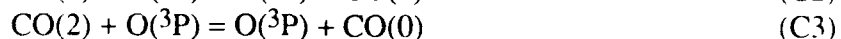
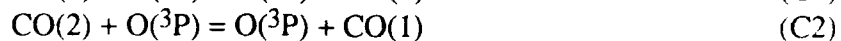
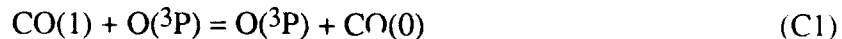
Figure B1. V-V energy transfer from CO(1) to N₂(0). Data from Mastrocinque et al. (Ref. B8), ■; Stephenson and Mosburg (Ref. B10), +; McLaren and Appleton (Ref. B4), □; Maricq et al., (Ref. B6), ○; Zittel and Moore (Ref. B2), /Green and Hancock (Ref. B9), ◆; Starr et al. (Ref. B11), ●; Sato et al. (Ref. B3), ×; von Rosenberg et al. (Ref. B5), Δ.

REFERENCES

- B1. R. L. Taylor, *Can. J. Chem.*, **52**, 1381 (1974).
- B2. P. F. Zittel and C. B. Moore, *Appl. Phys., Lett.*, **21**, 1972. (Room Temperature).
- B3. Y. Sato et al., *J. Chem. Phys.*, **50**, 1911 (1969). (1700-2700 K)
- B4. T.I. McLaren and J. P. Appelton, *Proceedings of the 8th Int. Shock Tube Symp.*, London, 1971, pp. 89-98. (2200-4000 K)
- B5. C.W. von Rosenberg et al., *J. Chem. Phys.*, **56**, 3230 (1972). (960-2200 K)
- B6. M. M. Maricq, E.A. Gregory, and C. J. Simpson, *Chem. Phys.*, **95**, 43 (1985). (70-300 K)
- B7. D.C. Allen and C.J. Simpson, *Chem. Phys.*, **45**, 203 (1980). (80-300 K)
- B8. G. Mastrocinque et al., *Chem. Phys. Lett.*, **39**(2), 348 (1976). (100-700 K)
- B9. W. H. Green and J. K. Hancock, *J. Chem. Phys.*, **59**, 4326 (1975). (298 K)
- B10. J. C. Stephenson and E. R. Mosburg, *J. Chem. Phys.*, **60**, (1974). (100-300 K)
- B11. D. F. Starr et al., *J. Chem. Phys.*, **61**, 5421 (1974). (100-650K)

APPENDIX C: V-T ENERGY TRANSFER FROM CO TO O(³P)

At altitudes above approximately 100-200 km, depending on the atmospheric model, ground state atomic oxygen becomes the dominant species. In some cases, such as the atmosphere described in Appendix F, there is a relatively high O atom number density, even in the mesosphere. CO vibrational and translational relaxation by ground state atomic oxygen can occur via the following pathways:



The temperature dependence of the rate of Eq. (C1), derived by Taylor (Ref. C1) in 1974, was

$$k_{1\text{ forward}} = 9.90\text{e-}8 \exp(-118.1\text{T}^{-1/3}) \quad (\text{C4})$$

This expression was based entirely on high temperature shock-tube data (Refs. C2, C3).

More recent laser-induced fluorescence (LIF) data between 265 and 389 K (Ref. C4) have been added to extend the temperature range and get an improved fit for k_1 . The data from Refs. C2-C4 are plotted in Figure C1.

$$k_{1\text{ forward}} = 2.82\text{e-}09 \exp(-75.4 \text{T}^{-1/3}) \quad (\text{C5})$$

$$k_{1\text{ reverse}} = 2.82\text{e-}09 \exp(-75.4 \text{T}^{-1/3} - 3083.7\text{T}^{-1}) \quad (\text{C6})$$

Using the harmonic oscillator approximation for vibrational energy level spacing in the Schwartz, Slawsky, and Herzfeld (SSH) (Ref. C5) treatment of vibrational relaxation rates, the CO(2-1) relaxation rate constant is estimated to be twice that for CO(1-0). No experimental information is available for the CO(2-0) relaxation rate, but it can be assumed that the rate constant will be much smaller than the (2-1) process since it involves transferring two quanta of energy per collision. The coefficients suggested for these upper level vibrational transitions are

$$k_{2\text{ forward}} = 5.64\text{e-}09 \exp(-75.4 \text{T}^{-1/3}) \quad (\text{C7})$$

$$k_{2\text{ reverse}} = 5.64\text{e-}09 \exp(-75.4 \text{T}^{-1/3} - 3045.6\text{T}^{-1}) \quad (\text{C8})$$

$$k_{3\text{ forward}} = 5.64\text{e-}10 \exp(-150.8 \text{T}^{-1/3}) \quad (\text{C9})$$

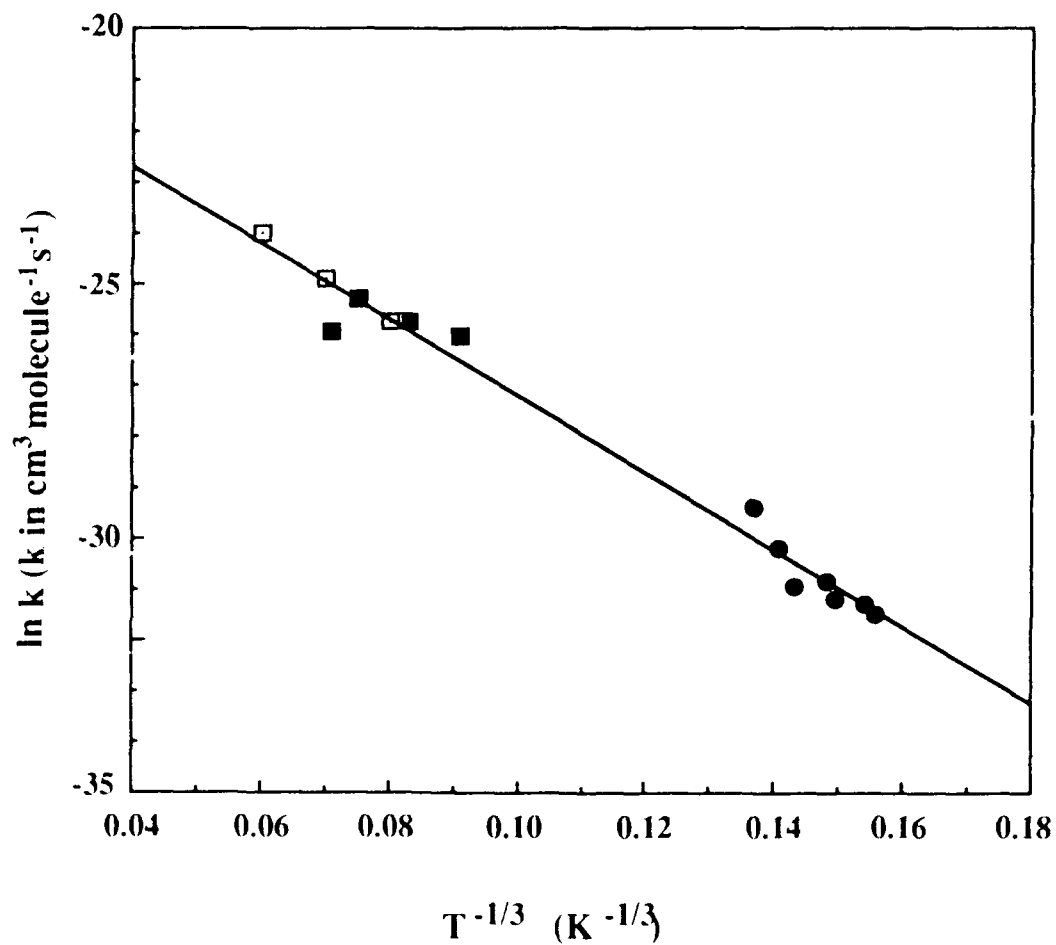


Figure C1. V-T energy transfer from CO(1) to O(³P). Data from Eckstrom (Ref. C3), ■: Lewittes et al. (Ref. C4), ●: Center (Ref. C2), □.

$$k_{3\text{reverse}} = 5.64e-10 \exp(-150.8T^{-1/3} - 6129.3T^{-1}) \quad (\text{C10})$$

The appropriate energy level spacing has been used for the temperature defect coefficients for the reverse reactions.

REFERENCES

- C1. R. L. Taylor, *Can. J. Chem.*, **52**(8) 1381 (1974).
- C2. R. E. Center, *J. Chem. Phys.*, **58**, 5230 (1973).
- C3. D.J. Eckstrom, *J. Chem. Phys.*, **59**, 2787 (1973).
- C4. M. E. Lewittes, C. D. Davis, and R. A. McFarlane, *J. Chem. Phys.*, **69**(5) 1952 (1978).
- C5. R. N. Schwartz, Z. I. Slawsky, and K. F. Herzfeld, *J. Chem. Phys.*, **20**, 1591 (1952).

APPENDIX D: V-T ENERGY TRANSFER FROM CO TO O₂ OR N₂

The following vibrational-to-translational energy transfer processes are possible for CO excited in the $v=1$ or $v=2$ levels, when CO collides with an atmospheric molecule



At the altitudes discussed in this review, the dominant molecular species, M, are N₂ or O₂.

Taylor (Ref. D1) reported the following temperature dependence for the rate constant of the reaction shown in Eq. (D1):

$$k_{\text{forward}} = 6.67\text{e-}8 \exp(-208.3T^{-1/3}) \quad (\text{D4})$$

It is difficult to distinguish the V-T contribution to the effective rate of relaxation in a mixture such as CO/N₂ or CO/O₂, where competitive V-V processes can occur to resonant or nearly resonant vibrational energy levels. Experimental data are often only available for the intermolecular V-V transfer rates since these are generally much faster than the V-T processes. However, the latter can be inferred from CO-atom energy transfer rates and from CO/CO V-T experimental data. Taylor used three primary references (Refs. D2-D4), which provided data for CO relaxation by Ar, and CO self-relaxation. The size of the error bars on these measurements is large (e.g., 43% in Ref. D1), so rates inferred by Taylor (and also in the present analysis) are roughly order of magnitude estimates. In Figure D1, the reported data points are plotted without error bars for the purpose of clarity. More recent but consistent experimental data on energy transfer from CO to He (Refs. D4, D5) are also included in Figure D1.

The temperature dependence function of the CO to M (M= O₂ or N₂) V-T rate will probably lie in between those for CO relaxation by He and by Ar, based on the relative masses of the collision partners. From Figure D1, it is evident that the CO self-relaxation rate also falls in between the He and Ar cases. Therefore, a linear Landau-Teller function was fitted to the Kovacs and Mack (Ref. D3) CO-CO data points and an average $\ln k$ intercept from the other data. The final temperature dependence is

$$k_{1 \text{ forward}} = 9.90\text{e-}09 \exp(-168.1T^{-1/3}) \quad (\text{D5})$$

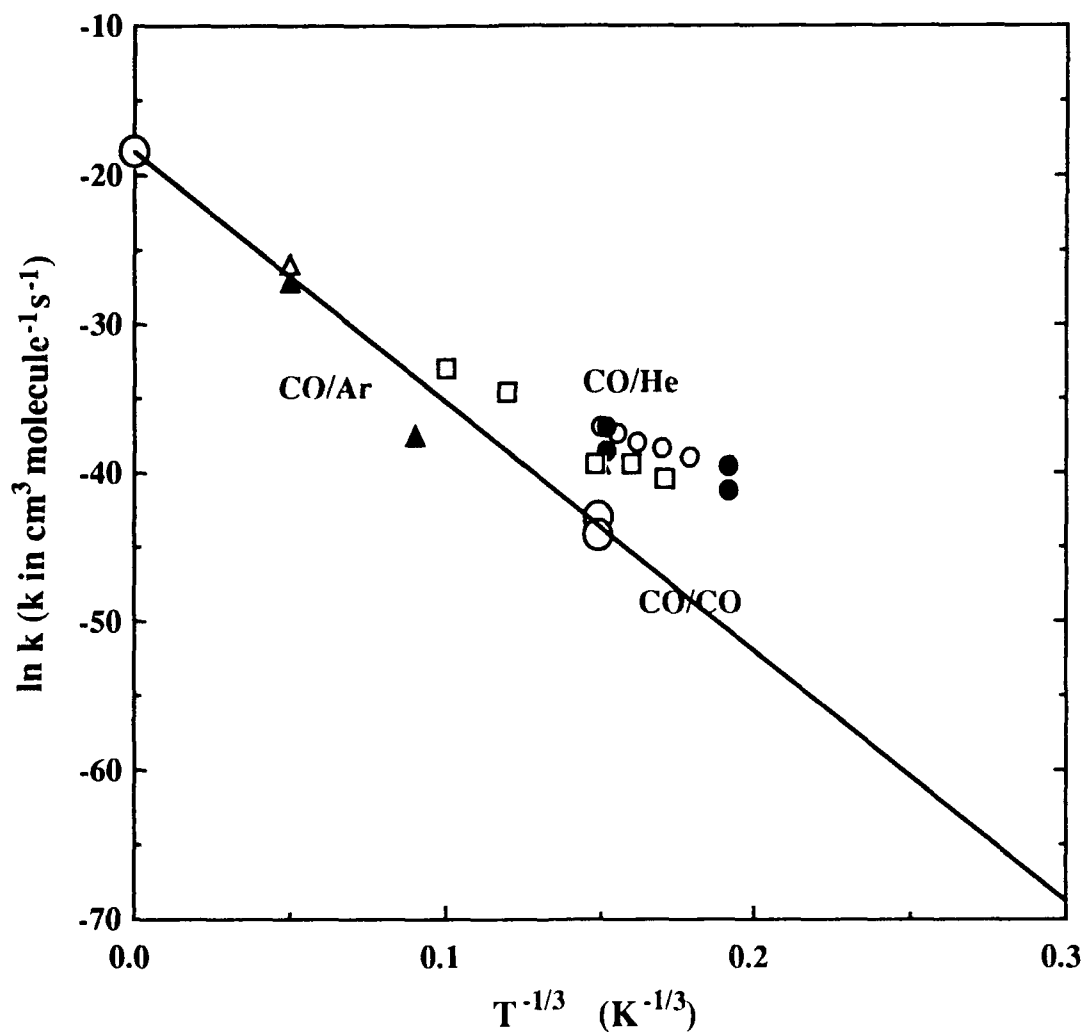


Figure D1. V-T energy transfer processes from CO(1). CO/Ar data from Millikan and White (Ref. D2), \blacktriangle . CO/He data from Millikan and White, (Ref. D2) \blacktriangle ; Maricq et al. (Ref. D7), \circ ; Schinke and Dierkson, (Ref. D6), \bullet ; Miller and Millikan (Ref. D5), \square . CO/CO data from Kovacs and Mack (Ref. D3), \circ .

Comparing the rate constant for the V-T process at any given temperature with that of the V-V CO to N₂ or O₂ rate constants, it is evident that the latter are considerably faster at low temperatures (e.g., 200 K). However, as the temperature increases, the difference in rate constants for the two types of processes decreases. For example, at 1500 K, the V-T relaxation of CO (v=1) by O₂ is approximately equal to the V-V relaxation by O₂.

Using the harmonic oscillator approximation in the Schwartz, Slawsky, and Herzfeld (SSH) theorem (Ref. D8), the rate constant for the (2-1) relaxation of CO [Eq (D2)] is estimated to be

$$k_{2 \text{ forward}} = 1.98\text{e-}08 \exp(-168.1T^{-1/3}) \quad (\text{D6})$$

The appropriate CO vibrational energy level spacing can be included in the $(-\Delta E/T)$ term for the reverse process. The (2-0) relaxation level should be a much less probable transition since it requires two quanta of energy to be transferred. Therefore, a scaled estimate for the (2-0) rate is

$$k_{3 \text{ forward}} = 1.98\text{e-}09 \exp(-336.2 T^{-1/3}) \quad (\text{D7})$$

Table 1 of the main text contains the full listing of rate coefficients for Eqs (D1)-(D3), including values for the less probable reverse processes.

REFERENCES

- D1. R. L. Taylor, *Can. J. Chem.*, **52**, 1381 (1974).
- D2. R.C. Millikan and D.R. White, *J. Chem. Phys.*, **39**, 3209 (1963).
- D3. M. A. Kovacs and M.A. Mack, *Appl. Phys. Lett.*, **20**, 487 (1972).
- D4. C. W. von Rosenberg et al., *Proceedings of the 13th Symp. Combustion*, The Combustion Institute, Pittsburg, PA, 1971, pp.89-98.
- D5. D.J. Miller and R. C. Millikan, *J. Chem. Phys.*, **53**, 3384 (1970).
- D6. R. Schinke and G.H. Diercksen, *J. Chem. Phys.*, **83**, 4520 (1985).
- D7. M. Maricq, E. Gregory et al., *Chem. Phys.*, **75**, 347 (1983).
- D8. R. N. Schwartz, Z. I. Slawsky, and K. F. Herzfeld, *J. Chem. Phys.*, 1591 (1952).

APPENDIX E: CO SPONTANEOUS EMISSION PROCESSES

The Einstein A coefficient for a transition from an upper level u to a lower level l is related to the sum-of-lines band strength S_{ul} by the following expression (Ref. E1):

$$A = \frac{8\pi c \nu^2 S_{ul}}{g_u} \frac{\exp[E_l/205.727]}{1 - \exp[-\nu/205.727]} \quad (\text{E1})$$

where the energy of the standard temperature (296 K) is 205.727 cm^{-1} . The appropriate units for the energy of the lower level, E_l , and the energy of the transition, ν , are cm^{-1} . The units for the speed of light, c , are cm/s . The degeneracy factor of the upper level, g_u , is dimensionless.

The 1987 Atmospheric Trace Molecule Spectroscopy (ATMOS) sum-of-lines band strengths (Ref. E2) for the CO vibrational level transitions are 9.81×10^{-18} (1-0), 5.70×10^{-22} (2-1), and 6.74×10^{-20} (2-0) in units of $\text{cm}^{-1} / \text{molecule}^{-1} \text{cm}^{-2}$ or cm/molecule (i.e., one Benedict) defined at 296 K. The calculated spontaneous emission rate constants are 33.98 s^{-1} , 64.43 s^{-1} , and 0.92 s^{-1} , respectively. The spacing of the vibrational levels is given in Table 2 of the main text.

The ATMOS band strengths are comparable to those in the HITRAN (Ref. E3) listing of the same year (1986). The HITRAN band strengths are 9.81×10^{-18} (1-0), 5.69×10^{-22} (2-1), and 7.52×10^{-20} (2-0) cm/molecule . Several papers that contain spectroscopic measurements and calculations pertaining to the (1-0) and (2-0) levels of CO are listed in Refs. E4-E7.

REFERENCES

- E1. R. D. Sharma, in *Modeling of the Atmosphere*, L. S. Rothman, ed., SPIE Vol. 928, 1988, p. 189.
- E2. L. R. Brown et al., *Appl. Opt.*, **26**, 5154 (1987).
- E3. L. S. Rothman et al., *Appl. Opt.*, **26**, 4058 (1987).
- E4. W.S. Benedict et al., *Astrophys. J.*, **135**, 277 (1962).
- E5. C. M. Sharp, *Astron. Astrophys., Suppl. Ser.*, **72**, 355 (1988).
- E6. G. Chandraiah and G. R. Hebert, *Can. J. Phys.*, **59**, 1367 (1981).
- E7. C. Chakerian Jr. and R. H. Tipping, *J. Mol. Spec.*, **99**, 431 (1983).

APPENDIX F: MODEL ATMOSPHERE USED FOR SHARC CALCULATIONS

ALT (KM)	TEMP (K)	N2	O2	O	CO2	CO	H2O	NO	O3	H	OH
50.0	270.6	0.1167E+17	0.4446E+16	0.800E+10	0.705E+13	0.993E+09	0.112E+12	0.220E+09	0.664E+11	0.328E+06	0.144E+08
52.0	269.0	0.13...17	0.352E+16	0.866E+10	0.556E+13	0.913E+09	0.873E+11	0.172E+09	0.384E+11	0.528E+06	0.132E+08
54.0	263.5	0.104E+17	0.278E+16	0.41E+10	0.439E+13	0.829E+09	0.682E+11	0.134E+09	0.255E+11	0.783E+06	0.119E+08
56.0	258.0	0.817E+16	0.219E+16	0.102E+11	0.345E+13	0.779E+09	0.526E+11	0.106E+09	0.161E+11	0.112E+07	0.116E+08
58.0	252.5	0.649E+16	0.171E+16	0.111E+11	0.271E+13	0.744E+09	0.410E+11	0.828E+08	0.112E+11	0.172E+07	0.114E+08
60.0	247.1	0.504E+16	0.135E+16	0.120E+11	0.203E+13	0.900E+09	0.335E+11	0.649E+08	0.730E+10	0.266E+07	0.113E+08
62.0	241.6	0.392E+16	0.105E+16	0.133E+11	0.158E+13	0.105E+10	0.260E+11	0.506E+08	0.480E+10	0.412E+07	0.118E+08
64.0	236.1	0.303E+16	0.812E+15	0.147E+11	0.122E+13	0.125E+10	0.204E+11	0.395E+08	0.310E+10	0.624E+07	0.124E+08
66.0	230.6	0.233E+16	0.624E+15	0.163E+11	0.936E+12	0.143E+10	0.151E+11	0.311E+08	0.180E+10	0.991E+07	0.126E+08
68.0	225.1	0.174E+16	0.477E+15	0.181E+11	0.715E+12	0.155E+10	0.139E+11	0.248E+08	0.870E+09	0.155E+08	0.125E+08
70.0	219.6	0.133E+16	0.362E+15	0.200E+11	0.542E+12	0.168E+10	0.792E+10	0.198E+08	0.380E+09	0.230E+08	0.124E+08
72.0	214.3	0.102E+16	0.273E+15	0.249E+11	0.408E+12	0.184E+10	0.575E+10	0.170E+08	0.170E+09	0.326E+08	0.111E+08
74.0	210.4	0.755E+15	0.203E+15	0.310E+11	0.304E+12	0.192E+10	0.387E+10	0.145E+08	0.820E+08	0.405E+08	0.989E+07
76.0	206.4	0.559E+15	0.150E+15	0.887E+10	0.225E+12	0.196E+10	0.261E+10	0.127E+08	0.420E+08	0.802E+07	0.802E+07
78.0	202.5	0.411E+15	0.110E+15	0.182E+11	0.165E+12	0.193E+10	0.168E+10	0.114E+08	0.300E+08	0.397E+08	0.589E+07
80.0	186.9	0.301E+15	0.807E+14	0.200E+11	0.121E+12	0.193E+10	0.106E+10	0.103E+08	0.400E+08	0.323E+08	0.433E+07
82.0	187.0	0.219E+15	0.586E+14	0.277E+11	0.879E+11	0.168E+10	0.658E+09	0.109E+08	0.730E+08	0.231E+08	0.245E+07
84.0	187.7	0.156E+15	0.424E+14	0.363E+11	0.635E+11	0.151E+10	0.359E+09	0.116E+08	0.900E+08	0.169E+08	0.139E+07
86.0	319.3	0.632E+14	0.163E+14	0.423E+11	0.456E+11	0.128E+10	0.203E+09	0.151E+08	0.860E+08	0.161E+08	0.628E+06
88.0	390.7	0.705E+14	0.112E+14	0.751E+11	0.319E+11	0.100E+10	0.114E+09	0.197E+08	0.680E+08	0.298E+08	0.227E+06
90.0	305.1	0.555E+14	0.118E+14	0.174E+12	0.224E+11	0.781E+09	0.614E+08	0.257E+08	0.490E+08	0.560E+08	0.821E+05
92.0	237.0	0.389E+14	0.113E+14	0.343E+12	0.157E+11	0.672E+09	0.344E+08	0.327E+08	0.340E+08	0.654E+08	0.308E+05
94.0	205.3	0.272E+14	0.906E+13	0.516E+12	0.110E+11	0.510E+09	0.184E+08	0.418E+08	0.200E+08	0.595E+08	0.116E+05
96.0	191.9	0.189E+14	0.780E+13	0.647E+12	0.764E+10	0.400E+09	0.105E+08	0.529E+08	0.120E+08	0.484E+08	0.422E+04
98.0	189.3	0.132E+14	0.523E+13	0.668E+12	0.533E+10	0.300E+09	0.634E+07	0.619E+08	0.610E+07	0.378E+08	0.150E+04
100.0	192.0	0.921E+13	0.345E+13	0.655E+12	0.372E+10	0.223E+09	0.377E+07	0.722E+08	0.300E+07	0.287E+08	0.566E+03
102.0	193.0	0.651E+13	0.243E+13	0.621E+12	0.260E+10	0.163E+09	0.234E+07	0.754E+08	0.140E+07	0.218E+08	0.262E+03
104.0	188.0	0.461E+13	0.143E+13	0.562E+12	0.182E+10	0.120E+09	0.142E+07	0.778E+08	0.660E+06	0.164E+08	0.142E+03
106.0	189.1	0.327E+13	0.119E+13	0.529E+12	0.128E+10	0.876E+08	0.842E+06	0.778E+08	0.290E+06	0.126E+08	0.868E+02
108.0	190.0	0.233E+13	0.605E+12	0.475E+12	0.902E+09	0.644E+08	0.481E+06	0.787E+08	0.130E+06	0.973E+07	0.575E+02
110.0	200.0	0.164E+13	0.362E+12	0.389E+12	0.631E+09	0.470E+08	0.256E+06	0.787E+08	0.514E+05	0.756E+07	0.403E+02
112.0	229.1	0.116E+13	0.225E+12	0.309E+12	0.385E+09	0.359E+08	0.137E+06	0.753E+08	0.189E+05	0.641E+07	0.300E+02
114.0	286.2	0.842E+12	0.116E+12	0.216E+12	0.246E+09	0.280E+08	0.669E+05	0.702E+08	0.765E+04	0.544E+07	0.225E+02
116.0	378.0	0.629E+12	0.664E+11	0.153E+12	0.162E+09	0.225E+08	0.336E+05	0.702E+08	0.333E+04	0.446E+07	0.173E+02
118.0	419.0	0.479E+12	0.449E+11	0.130E+12	0.111E+09	0.184E+08	0.260E+05	0.660E+08	0.156E+04	0.348E+07	0.137E+02
120.0	469.3	0.373E+12	0.339E+11	0.128E+12	0.775E+08	0.153E+08	0.204E+05	0.615E+08	0.767E+03	0.251E+07	0.103E+02
122.0	488.4	0.295E+12	0.236E+11	0.993E+11	0.556E+08	0.126E+07	0.163E+05	0.560E+08	0.442E+03	0.214E+07	0.825E+01
124.0	527.5	0.237E+12	0.163E+11	0.884E+11	0.407E+08	0.106E+08	0.133E+05	0.498E+08	0.254E+03	0.182E+07	0.672E+01
126.0	555.2	0.193E+12	0.139E+11	0.796E+11	0.304E+08	0.904E+07	0.109E+05	0.435E+08	0.147E+03	0.151E+07	0.559E+01
128.0	585.9	0.159E+12	0.108E+11	0.692E+11	0.231E+08	0.775E+07	0.913E+04	0.378E+08	0.847E+02	0.120E+07	0.473E+01
130.0	619.3	0.133E+12	0.868E+10	0.624E+11	0.178E+08	0.683E+07	0.771E+04	0.326E+08	0.490E+02	0.912E+06	0.398E+01
132.0	645.7	0.112E+12	0.713E+10	0.516E+11	0.139E+08	0.581E+07	0.657E+04	0.278E+08	0.330E+02	0.808E+06	0.340E+01
134.0	691.0	0.746E+11	0.599E+10	0.519E+11	0.109E+08	0.500E+07	0.563E+04	0.245E+08	0.230E+02	0.703E+06	0.290E+01
136.0	706.2	0.808E+11	0.503E+10	0.472E+11	0.871E+07	0.432E+07	0.488E+04	0.214E+08	0.160E+02	0.598E+06	0.252E+01
138.0	729.3	0.695E+11	0.430E+10	0.430E+11	0.700E+07	0.376E+07	0.425E+04	0.187E+08	0.106E+02	0.493E+06	0.218E+01
140.0	754.4	0.601E+11	0.370E+10	0.403E+11	0.567E+07	0.330E+07	0.372E+04	0.163E+08	0.720E+01	0.388E+06	0.191E+01

APPENDIX F (CONT.): MODEL ATMOSPHERE USED FOR SHARC CALCULATIONS

ALT (KM)	TEMP (K)	N2	O2	O	TOTAL NUMBER DENSITY (MOLEC./CM3)									
					CO2	CO	H2O	NO	O3	H	OH			
142.0	796.3	0.523E+11	0.332E+10	0.379E+11	0.462E+07	0.291E+07	0.328E+04	0.141E+08	0.540E+01	0.337E+06	0.168E+01			
144.0	807.6	0.457E+11	0.294E+10	0.448E+11	0.380E+07	0.257E+07	0.290E+04	0.124E+08	0.400E+01	0.292E+06	0.149E+01			
146.0	830.1	0.401E+11	0.263E+10	0.330E+11	0.314E+07	0.229E+07	0.238E+04	0.110E+08	0.300E+01	0.247E+06	0.132E+01			
148.0	855.3	0.353E+11	0.215E+10	0.293E+11	0.261E+07	0.205E+07	0.231E+04	0.955E+07	0.220E+01	0.202E+06	0.118E+01			
150.0	877.6	0.312E+11	0.205E+10	0.278E+11	0.218E+07	0.185E+07	0.207E+04	0.819E+07	0.166E+01	0.160E+06	0.106E+01			
160.0	976.8	0.177E+11	0.126E+10	0.204E+11	0.944E+06	0.109E+07	0.126E+04	0.412E+07	0.580E+00	0.713E+05	0.644E+00			
170.0	1080.1	0.107E+11	0.808E+09	0.162E+10	0.444E+06	0.700E+06	0.822E+03	0.211E+07	0.200E+00	0.345E+05	0.416E+00			
180.0	1153.9	0.674E+10	0.542E+09	0.125E+10	0.222E+06	0.470E+06	0.560E+03	0.122E+07	0.710E-01	0.171E+05	0.282E+00			
190.0	1225.8	0.438E+10	0.303E+09	0.118E+10	0.116E+06	0.298E+06	0.395E+03	0.804E+06	0.250E-01	0.800E+04	0.199E+00			
200.0	1284.8	0.292E+10	0.272E+09	0.875E+10	0.628E+05	0.195E+06	0.287E+03	0.530E+06	0.860E-02	0.408E+04	0.144E+00			
210.0	1339.9	0.199E+10	0.224E+09	0.741E+10	0.348E+05	0.130E+06	0.213E+03	0.349E+06	0.470E-02	0.202E+04	0.108E+00			
220.0	1382.4	0.137E+10	0.141E+09	0.637E+10	0.196E+05	0.907E+05	0.161E+03	0.230E+06	0.260E-02	0.105E+04	0.810E-01			
230.0	1425.0	0.960E+09	0.113E+10	0.548E+10	0.114E+05	0.657E+05	0.124E+03	0.152E+06	0.140E-02	0.610E+03	0.624E-01			
240.0	1456.6	0.678E+09	0.865E+08	0.470E+10	0.665E+04	0.489E+05	0.960E+02	0.100E+06	0.760E-03	0.315E+03	0.486E-01			
250.0	1486.1	0.483E+09	0.648E+08	0.413E+10	0.388E+04	0.380E+05	0.760E+02	0.656E+05	0.480E-03	0.174E+03	0.380E-01			
260.0	1512.0	0.346E+09	0.519E+08	0.364E+10	0.229E+04	0.302E+05	0.600E+02	0.431E+05	0.240E-03	0.103E+03	0.302E-01			
270.0	1535.0	0.249E+09	0.417E+08	0.319E+10	0.138E+04	0.242E+05	0.480E+02	0.283E+05	0.140E-03	0.581E+02	0.242E-01			
280.0	1555.1	0.181E+09	0.311E+08	0.283E+10	0.634E+03	0.194E+05	0.390E+02	0.186E+05	0.810E-04	0.319E+02	0.194E-01			
290.0	1572.0	0.131E+09	0.264E+08	0.252E+10	0.507E+03	0.158E+05	0.320E+02	0.122E+05	0.470E-04	0.178E+02	0.158E-01			
300.0	1587.6	0.959E+08	0.204E+08	0.243E+10	0.310E+03	0.129E+05	0.260E+02	0.800E+02	0.270E-04	0.973E+01	0.128E-01			